ACS APPLIED MATERIALS & INTERFACES

RESEARCH ARTICLE

www.acsami.org

Facile Preparation of Nitrogen-Doped Few-Layer Graphene via Supercritical Reaction

Wen Qian,[†] Xu Cui,[†] Rui Hao,[†] Yanglong Hou,*[,†] and Zhiyong Zhang*[,‡]

[†]Department of Advanced Materials and Nanotechnology, College of Engineering, and [‡]Key Laboratory for the Physics and Chemistry of Nanodevices and Department of Electronics, Peking University, Beijing 100871, China

Supporting Information

ABSTRACT: To achieve the applications of graphene, the modulation of its electrical properties is of great significance. The element doping might give a promising approach to produce fascinating properties of graphene. Herein we report a facile chemical doping method to obtain nitrogen-doped (N-doped) few-layer graphene sheets through supercritical (SC) reaction in acetonitrile at temperature as low as 310 °C, using expanded graphite as starting material. X-ray photoelectron spectroscopy analysis revealed that the level of nitrogen-doping (N-doping) increased from 1.57 to 4.56 at % when the reaction time was tuned from 2 to 24 h. Raman spectrum confirmed that the resulting N-doped few-layer graphene by SC reaction maintain high quality without any significant structural defects. Electrical measurements indicated that N-doped few-layer graphene sheets exhibit a typical *n*-type field-dependent behavior, suggesting the N-doping into the lattice of graphene. This work provides a convenient chemical route to the scalable production of N-doped graphene for potential applications in nanoelectronic devices.

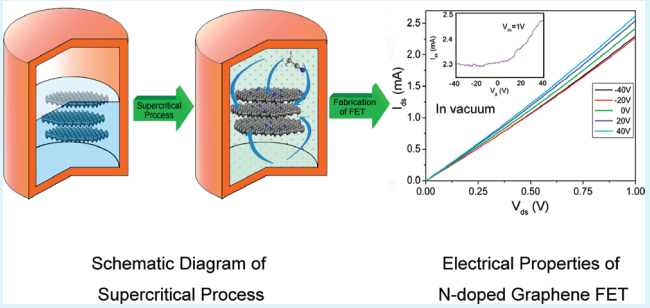

KEYWORDS: N-doped graphene, supercritical reaction, *n*-type FET, high quality, few-layer, chemical doping

1. INTRODUCTION

Graphene, as a perfect freestanding two-dimensional material, has been predicted to have numerous applications in transparent electrodes, field effect transistors (FETs), ultrasensitive sensors and composites, due to its unique electronic transport property, thermal conductivity and high mechanical strength.[1−7] It is well known that graphene is a unique zero band-gap semiconductor with a carrier mobility as high as 2×10^5 cm^2/V s, which is an order of magnitude higher than that of silicon wafers,[8] making it a promising candidate for high-frequency applications in next generation nanoelectronics. However, most of the as-made graphene FETs are *p*-type because of the adsorption of oxygen or water in air. To realize graphene-based integrated circuits with complement FETs that possess the advantages of high noise immunity and low static power consumption, both *n*-type and *p*-type devices are certainly required. Physical or chemical doping with nitrogen in the graphene lattice is an effective method to prepare N-doped graphene. Up to now, a variety of studies of N-doped graphene- or carbon nanotubes- based devices have been presented.[9−19] Recently, Dai et al. reported a physical doping method to prepare N-doped graphene nanoribbons by high-power electrical joule heating,[11] afterwards, they also reported a chemical doping method to obtain N-doped graphene by thermal annealing of reduced graphene oxide.[12] Liu et al. reported a chemical vapor deposition method to synthesize N-doped graphene.[13] However, all the reported methods almost have two characteristics: one is selecting ammonia as nitrogen source and the other is high reaction temperature in the gas atmosphere. In addition, theoretical simulations have predicted that compared with monolayer graphene, bilayer or few-layer graphene may be a better choice for fabricating FETs because of lower noise and higher reliability.[20] Therefore, utilizing a simple and mild doping method to obtain high-quality N-doped few-layer graphene is prerequisite to maximizing the potential application in next generation nanoelectronic devices. Very recently, 5 wt % N-doped graphene sheets were prepared through a hydrothermal reduction of graphite oxide in the presence of hydrazine and ammonia.[21] Our group has previously reported that high-quality graphene sheets can be produced by a solvothermal-assisted exfoliation reaction in acetonitrile (ACN), using expanded graphite (EG) as starting material.[22] It is worth noting that ACN is also an ideal supercritical (SC) fluid for its approachable SC conditions with a critical temperature (T_C) of 272.5 °C and critical pressure (P_C) of 4.85 MPa.[23] As is well known, the most common SC fluid, SC CO_2, has been widely utilized to intercalate tightly-stacked layered materials such as clay and graphite.[24,25] It is expected that SC ACN can also penetrate the interlayers of graphene and makes nitrogen atoms bonded in the lattice of graphene.

Received: January 19, 2011
Accepted: June 6, 2011
Published: June 06, 2011

dx.doi.org/10.1021/am200479d | *ACS Appl. Mater. Interfaces* 2011, 3, 2259–2264

Scheme 1. Schematic Illustration of N-Doped Graphene Sheets Prepared via SC Reaction with ACN at 310 °C: (a) Few-layer Graphene Sheets Were Obtained by Solvothermal-Assisted Exfoliation Process and Centrifugation, And Then Were Mixed with ACN in Corundum-Lined Autoclave (b) N-Doped Graphene Sheets Were Formed after SC Reaction with ACN at 310 °C for Designated Time

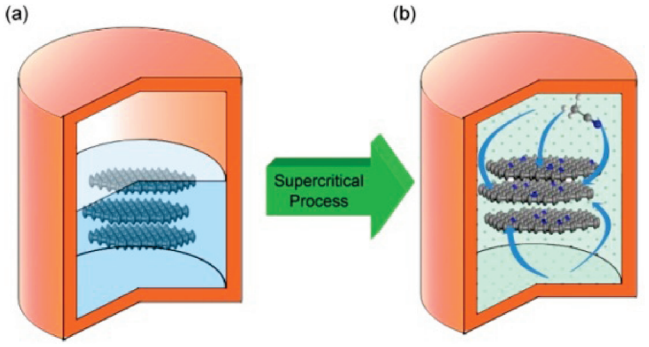

In this work, we report that N-doped graphene sheets can be readily prepared by a SC reaction in ACN at the relatively low temperature of about 310 °C. Nitrogen atoms, which act as electron donors, can be partially doped into the graphene lattice. As a result, the level of nitrogen-doping (N-doping) in graphene sheets can be tuned by varying the reaction time. Electrical measurements show that the N-doped graphene exhibits *n*-type field-dependent behavior. The procedure described here offers a simple and large-scale method to obtain high-quality N-doped graphene which could have more potential applications in nanoelectronics.

2. EXPERIMENTAL SECTION

2.1. Supercritical Process to Prepare N-Doped Graphene. Graphene sheets were prepared by a solvothermal-assisted exfoliation process in ACN using EG as starting material.[22] The resulting solution was centrifuged at 500 rpm for 30 min to remove a small amount of thick graphite sheets in the solution. The supernatant was then centrifuged again at 15 000 rpm for 7 min to collect few-layer graphene sheets (a yield around 10−12 wt %) for further doping reaction. The resulting few-layer graphene sheets (2 mg) were dispersed in ACN (25 mL), and the mixture was transferred to a corundum-lined autoclave (50 mL). The autoclave was heated to 310 °C and remained at this temperature for various time intervals from 2 h - 24 h, which maintained an environment of SC fluid within the autoclave. After the SC reaction, the resulting N-doped graphene sheets formed a brown suspension due to ACN polymerization, which was centrifuged at 15 000 rpm to remove the original ACN, and were redispersed in fresh ACN by sonicating for 30 min, forming a gray suspension, as the intrinsic color of graphene. To remove physically absorbed nitrogen on the graphene sheets, the annealing of resulting graphene was carried out in a tube furnace at 200 °C for 30 min with the flowing of Ar under ~2 Torr.

2.2. Fabrication of Graphene FET Devices. Bottom-gated graphene FET devices were prepared by spin-coating several drops of the graphene suspension described above onto a silicon wafer substrate insulated by a 500 nm thick silicon oxide layer. By means of electron beam lithography technique, a 10 nm Ti/40 nm Au metal pattern was deposited as source/drain contacts, followed by lift-off, finally forming an individual N-doped graphene FET device. Before measuring the electrical properties of N-doped graphene FETs, the vacuum system was pumped to 1×10^{-7} Torr and then maintained at 200 °C for 12 h to remove the physically adsorbed N and O atoms.

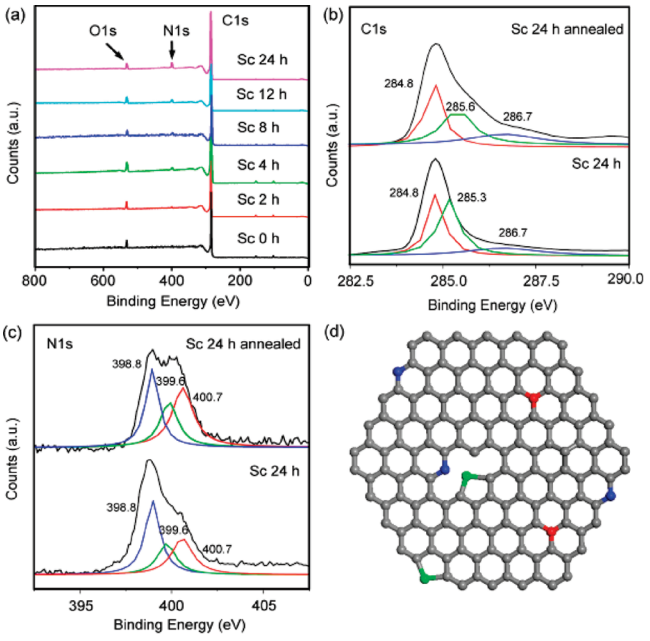

Figure 1. XPS spectra and schematic representation of N-doped graphene sheets prepared by SC reaction. (a) XPS spectra of N-doped graphene obtained by SC reaction from 0 to 24 h, respectively. (b) C1s spectra of N-doped graphene obtained at 24 h and its annealed samples. The C1s peak can be fitted by three Lorentzian peaks at 284.8, 285.3, and 286.7 eV, which are labeled by red, green and blue lines, respectively. (c) N1s spectra of N-doped graphene obtained at 24 h and its annealed samples; The N1s peak can be fitted by three Lorentzian peaks at 398.8, 399.6, and 400.7 eV, which are labeled by blue, green, and red lines, respectively. (d) Schematic representation of the N-doped graphene. The gray, blue, green and red spheres represent C, "pyridinic" N, "pyrrolic" N, and "graphitic" N atoms, respectively.

2.3. Structural and Properties Characterization. The Raman spectrum was collected on a RENISHAW inVia Confocal Laser Micro-Raman spectrometer using an Ar^+ laser with 514.5 nm at room temperature. X-ray photoelectron spectroscopy (XPS) measurements were carried out using Imaging Photoelectron Spectrometer (Kratos, Axis Ultra) which used Al (K_α) radiation as a probe, the XPS data were analyzed by using the fitting of Lorentzian peaks. All electrical measurements were carried out with a Keithley 4200 semiconductor characterization system in air/vacuum at room temperature. The morphology and crystal structure of N-doped graphene were characterized by Philips Tecnai F30 field-emission transmission electron microscope (FETEM) and the electron diffraction (ED) was operated with the accelerating voltage of 300 kV. The shape of N-doped graphene FET device was observed by HITACHI S-4800 field-emission scanning electron microscope (FESEM).

3. RESULTS AND DISCUSSION

Scheme 1 illustrates the SC reaction process used to produce the N-doped graphene sheets. According to the phase diagram of ACN,[26,27] as the reaction temperature and pressure are kept above the T_C and P_C, ACN will exhibit as SC fluid which possesses the properties of both gaseous dissipation and liquid fluidity. Therefore, in the present system, ACN can not only penetrate the interlayers of graphene sheets with high diffusivity but also disperse the graphene sheets as liquid solvent.[25,28] It is well known that the cyano group of ACN is composed of one σ bond and two π bonds, under certain reaction conditions, such as high temperature and high pressure,[29,30] or catalyst addition,[31] the

cyclotrimerization of cyano group will form a 1,3,5-triazine ring. Herein, the reaction temperature and pressure of SC environment induce the insertion of the ACN molecules into the interlayers of graphene, and promote the activation of π bonding, making it react with the dangling bonds of carbon atoms. After a long period of reaction, the N atoms can enter into the graphene lattice, and form covalent bonds with carbon atoms.[32] It is suggested that the formation of C−N bond should occur primarily at the edges, vacancies, and topological defect sites in the lattice of graphene which are electronic or chemical active.[11]

High-resolution XPS spectra of the few-layer graphene prepared by SC reaction from 0 h to 24 h further confirmed the presence of various N-doping levels, as shown in Figure 1a−d. The peaks at 284.8, 398.8, and 531.9 eV (Figure 1a) can be assigned to C1s, N1s, and O1s, respectively. In the pristine graphene (Figure 1a, SC 0h), N1s peak cannot be observed, whereas in the N-doped graphene (Figure 1a, SC 2−24h), the atomic percentage of N increases from 1.57 to 2.39, 3.02, 3.80, and 4.56 at %, respectively, with the increase of reaction time from 2 to 4, 8, 12, and 24 h. The results demonstrate that the N-doping level in graphene sheets can be regulated by tuning the reaction time. When the reaction time was extended over 24 h, N-doping level would not increase any more with a limit about 4.56 at %. The C1s spectra of pristine graphene (SC 0h) and N-doped graphene (SC 24h and its annealed sample) were investigated, as shown in Figure S1 in the Supporting Information and Figure 1b. For pristine graphene, the deconvoluted three peaks at 284.8 eV, 285.7 eV and 288.7 eV, can be assigned to C−C bonding, C−OH and O═C−OH functional groups.[33−35] For the N-doped graphene, the main peak at 284.8 eV is still assigned to the graphite-like sp^2 C,[36,37] but the small peaks at 285.3 eV and 286.7 eV reflect the different bonding structures of the C−N, corresponding to N-sp^2 C and N-sp^3 C bonds, which is due to the substitution of the N atoms at defects and the edge of the graphene lattice.[32,33] In the N1s spectrum of graphene obtained at 24 h, there are three different types of N bonding (Figure 1c,d). The peak at 398.8 eV is attributed to pyridinic-type N, and the peak at 399.6 eV corresponds to pyrrolic-type N.[12,37] These two kinds of N atoms are usually considered to be located in a π-conjugated system and contribute to the π system with one or two electrons, respectively. The peak at 400.7 eV is assigned to "graphitic" N, which refers to C atoms in the graphitic lattice replaced by N atoms. Detailed N binding configuration was listed in Table S1 in the Supporting Information, including the atomic percentage of pyridinic N, pyrrolic N and graphitic N at different reaction times. To fully remove the physisorbed nitrogen, our sample was annealed at 200 °C, and afterwards the percentage of N atoms decreased to 3.35 at %, which should primarily consisted of "pyrrolic" N and "graphitic" N as shown in Figure 1c (top). It can be primarily concluded that nitrogen has been effectively doped in the crystalline lattice of graphene after the SC reaction in the presence of ACN. In addition, the O1s peak basically arises from two parts; one is due to the oxygen atoms existing at the graphene edges, vacancies, or defects, and the other is ascribed to water adsorbed on the graphene surface. The former part was decreased from 6.91 to 2.51 at % while the reaction time increased from 8 to 24 h (Figure 1a), indicating that some of oxygen atoms in the graphitic lattice might have been reduced or replaced by nitrogen atoms during the reaction. The latter part can be completely removed by vacuum annealing at 200 °C for 12 h.

Transmission electronic microscope (TEM) and electron diffraction (ED) analyses were further employed to investigate

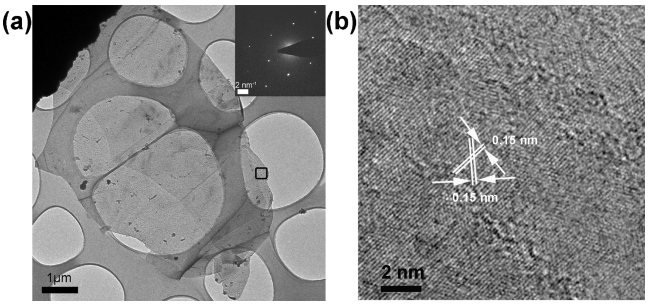

Figure 2. (a) TEM image of N-doped few-layer graphene sheets and the corresponding ED (inset). (b) the enlarged high-resolution TEM image of boxed area in (a).

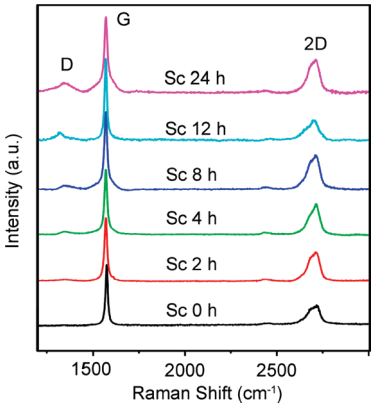

Figure 3. Raman spectra of few-layer graphene prepared by SC reaction with ACN at the reaction times from 0 to 24 h.

the morphology and crystal structure of N-doped few-layer graphene prepared by SC reaction with ACN for 24 h. Figure 2a is a typical TEM image of crumpled graphene sheets deposited on a lacey carbon film, which are several micrometers in size and have folded edges. The corresponding ED pattern (inset) exhibits a typical six-fold symmetry diffraction pattern which is ascribed to graphite/graphene. The enlarged high resolution image of boxed area in Figure 2a was shown in Figure 2b. It is interesting to identify hexagonal lattice structure of graphene, indicating that the C−C bond length is about 0.15 nm in two-dimensional plane, even though at the accelerating voltage of 200 kV. The distinctive lattice structure unambiguously confirmed the resulting N-doped graphene sheets still remain high quality without significant defects after SC reaction process with ACN for 24h.

Raman spectroscopy has been accepted as a nondestructive, purely optical, and high-throughput technique for evaluating the structure defects, number of layers, and doping level of graphene. The Raman spectrum of graphene is dominated by three main features, G, D, and 2D Raman modes, each has different physical origin.[38,39] The peak at ~1580 cm^{-1} (G band), arising from the emission of zone-centre optical phonons, corresponds to the doubly degenerate E_{2g} mode of graphite related to the vibration of sp^2-bonded C; the peak at ~1350 cm^{-1} (D band) is assigned to the presence of specific defects, vacancies and in-plane heteroatom.[34] The peak at ~2700 cm^{-1} (2D) is the second order of zone-boundary phonons. Figure 3 shows the Raman spectra of few-layer N-doped graphene prepared by SC reaction

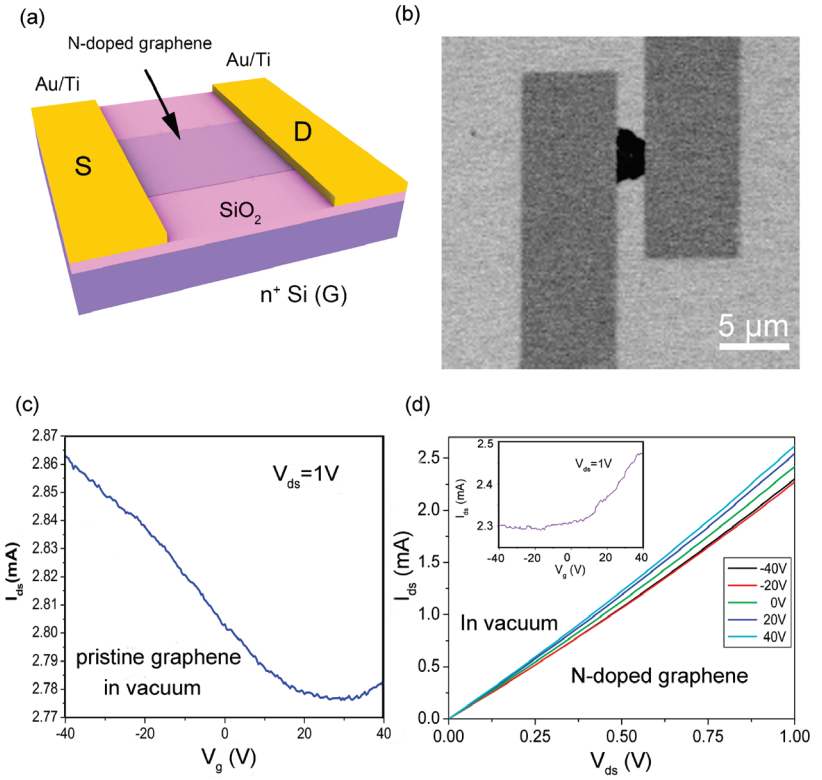

Figure 4. Electrical properties of N-doped graphene device. (a) Schematic illustration of the graphene device with SiO_2/Si substrate as the gate. (b) FESEM image of N-doped few-layer graphene device. (c) The typical transfer characteristics of pristine graphene device recorded in vacuum at bias V_{ds} = 1 V. (d) $I_{ds}-V_{ds}$ curves of N-doped graphene under different V_g recorded in vacuum. V_g = −40, −20, 0, 20, and 40 V from bottom to top. The inset is the transfer characteristics of at bias V_{ds} = 1 V.

with ACN while the reaction time varies from 0 to 24 h. In Figure 3, note that with the increase of the reaction time from 0 to 2, 4, 8, 12, and 24 h, the ratio of I_D/I_G also slightly increases to some extent from 0.021 to 0.029, 0.051, 0.052, 0.080, and 0.127, respectively. The activation of the weak D peak in the N-doped graphene samples is due to the increased defects and heteroatoms,[39] which should include the breaking of C−C sp^2 bonds and the formation of C−N sp^3 bonds in graphene. The results of Raman spectra supply the evidence that the SC reactions with ACN can introduce defects to the surface of graphene; On the other hand, XPS spectra proved the existence of "pyridinic *N*", "pyrrolic *N*" and "graphitic *N*", therefore, it can be concluded that nitrogen atoms have reacted with carbon atoms on the defects and vacancies, or replaced the carbon atoms in the lattice of graphene. It is also worth noting that all of these Raman spectra of N-doped graphene only have invisible or weak D bands, suggesting that the graphene sheets still remain high crystallinity.

To investigate how the N-doping process affects the electronic properties of graphene, the single sheet, bottom-gated FET devices of both pristine graphene and N-doped graphene were fabricated with Au/Ti metals as source-drain contacts (Figure 4a, b). The graphene, bridging the source and drain electrodes, served as the conducting channel. It is well known that the pristine graphene is a zero-gap semiconductor. The band structure of graphene exhibits the valence band and the conduction band intersecting at two equivalent points (K and K′) in the reciprocal space, exhibiting an excellent conductivity. However, due to its physisorbed molecular oxygen, the pristine graphene usually shows *p*-type behavior, which was recorded both in vacuum (Figure 4c) and in air (see Figure S2 in the Supporting Information). Figure 4d show the typical source-drain current (I_{ds}) vs the source-drain voltage (V_{ds}) curves at different gate voltage (V_g) of individual N-doped graphene obtained from the SC reaction in the presence of ACN at 310 °C for 24 h, which was also measured both in vacuum (Figure 4d) and in air (see Figure S3 in the Supporting Information). It is worth noting that the measuring system has been pumped to 1×10^{-7} Torr, and then the devices were maintained at 200 °C for 12 h before the measurements, therefore all of the physically adsorbed N and O atoms on the surface of graphene have been completely removed out. Only chemically bonded N atoms could be stably existed in the lattice of graphene. The changing $I_{ds}-V_{ds}$ characteristics with the function of V_g demonstrates that the output properties of the N-doped graphene device can be effectively modulated by applying different gate voltage. The transfer properties of the N-doped graphene device have also been examined (see Figure 4d and the inset to Figure S3 in the Supporting Information) by applying V_g of up to ±40 V, I_{ds} decreases with the decrease of V_g from +40 V to −40 V, recorded at V_{ds} = 1 V both in vacuum and in air. Note that Dirac Point position was shifted from $V_{gs} \gtrsim 20$ V for pristine graphene (Figure 4c and Figure S1 in the Supporting Information) to $V_{gs} \lesssim -20$ V for N-doped graphene (Figure 4d and the inset in Figure S2 in the Supporting Information), confirming a conversion from *p*-type to *n*-type of FETs. The above results demonstrated that substituted N atoms introduce strong electron donors to the density of states near the Fermi energy level, modulating the electrical

structure of graphene. Although the additional electrons could be injected into graphene lattice which would induce higher carrier density, it would also introduce structural defects to some certain extent. Therefore, the carrier mobility will vary significantly depending on the doping level and carrier density.[10] In addition, the sheet resistance of the N-doped graphene is as low as ~300 Ω/sq, indicating that the N-doped graphene prepared by the SC reaction for 24 h is still of high quality without any significant defects, which is consistent with the results of Raman spectra. The relatively low I_{on}/I_{off} ratio (1.10−1.15) indicates that the bandgap between valence and conduction has not been effectively opened. Considering graphene nanoribbons[11] and nanomesh[40,41] possess high I_{on}/I_{off} ratio, therefore, if the resulting N-doped graphene sheets produced by the SC reaction could be cut into the shape of nanoribbon or nanomesh in the post-treatment technique, the bandgap can be opened up and at the same time the low resistance will be maintained due to the high quality of N-doped graphene. It is also worth mentioning that more than ten of graphene-based FET devices were fabricated, and each single graphene device exhibited the similar characteristics of *n*-type field-dependent behavior, as shown in Figures S4 and S5 in the Supporting Information, also suggesting that all of resulting graphene prepared by the SC reaction are N-doped graphene sheets. This method provides an effective route to the production of N-doped few-layer graphene sheets and fabrication of *n*-type devices.

4. CONCLUSIONS

In summary, we reported a simple, mild, and effective method to prepare N-doped graphene through a SC reaction with ACN at a low temperature of 310 °C. Detailed investigation of resulting graphene by XPS, HRTEM, and Raman spectra revealed that the N-doping level can be tuned by varying reaction times from 2 to 24 h, and maximum N-doping level can reach up to 4.56 at %. The resulting N-doped graphene still keep high crystal structure without significant defects after SC reaction process for 24 h. Furthermore, electrical properties of the N-doped graphene devices were measured, which show *n*-type FET behaviour, indicating that the N-doping can modulate its electrical properties. It is expected that N-doped graphene sheets could be potentially applied to the areas of transistors, sensors, fuel cells, and supercapacitors in the future.

■ ASSOCIATED CONTENT

Supporting Information. Additional information about C1s of Sc 0h graphene sample, the typical transfer characteristics of pristine graphene and N-doped graphene measured in air, and two additional N-doped graphene FETs devices measured in a vacuum. This material is available free of charge via the Internet at http://pubs.acs.org/.

■ AUTHOR INFORMATION

Corresponding Authors

*E-mail: hou@pku.edu.cn; zyzhang@pku.edu.cn.

■ ACKNOWLEDGMENT

This work was partially supported by the National Nature Science of Foundation of China (NSFC) (21051002, 20941003), the National Basic Research Program of China (2010CB934601), the Doctoral Program (20090001120010) and New Century Talent (NCET-09-0177) of the Education Ministry of China, Yok Ying Tung Found (122043), Beijing Outstanding Talent Program (2009D013001000013) and New Star Program of BCST (2008B02). W. Qian acknowledges the fellowship supported by China Postdoctoral Science Foundation. We also thank for Prof. B. Han at Institute of Physics (CAS) and Mr. I. Chaudhury at University of Rochester for their kind help.

■ REFERENCES

(1) Novoselov, K. S.; Geim, A. K.; Morozov, S. V.; Jiang, D.; Zhang, Y.; Dubonos, S. V.; Grigorieva, I. V.; Firsov, A. A. *Science* **2004**, *306*, 666–669.
(2) Novoselov, K. S.; Geim, A. K.; Morozov, S. V.; Jiang, D.; Katsnelson, M. I.; Grigorieva, I. V.; Dubonos, S. V.; Firsov, A. A. *Nature* **2005**, *438*, 197–200.
(3) Berger, C.; Song, Z. M.; Li, X. B.; Wu, X. S.; Brown, N.; Naud, C.; Mayou, D.; Li, T. B.; Hass, J.; Marchenkov, A. N.; Conrad, E. H.; First, P. N.; de Heer, W. A. *Science* **2006**, *312*, 1191–1196.
(4) Ang, P. K.; Chen, W.; Wee, A. T. S.; Loh, K. P. *J. Am. Chem. Soc.* **2008**, *130*, 14392–14393.
(5) Stankovich, S.; Dikin, D. A.; Dommett, G. H. B.; Kohlhaas, K. M.; Zimney, E. J.; Stach, E. A.; Piner, R. D.; Nguyen, S. T.; Ruoff, R. S. *Nature* **2006**, *442*, 282–286.
(6) Wang, X.; Zhi, L. J.; Mullen, K. *Nano Lett.* **2008**, *8*, 323–327.
(7) Geim, A. K.; Novoselov, K. S. *Nat. Mater.* **2007**, *6*, 183–191.
(8) Du, X.; Skachko, I.; Barker, A.; Andrei, E. Y. *Nat. Nanotechnol.* **2008**, *3*, 491–495.
(9) Li, N.; Wang, Z. Y.; Zhao, K. K.; Shi, Z. J.; Gu, Z. N.; Xu, S. K. *Carbon* **2010**, *48*, 255–259.
(10) Lherbier, A.; Blase, X.; Niquet, Y. M.; Triozon, F.; Roche, S. *Phys. Rev. Lett.* **2008**, *101*, 036808.
(11) Wang, X. R.; Li, X. L.; Zhang, L.; Yoon, Y.; Weber, P. K.; Wang, H. L.; Guo, J.; Dai, H. J. *Science* **2009**, *324*, 768–771.
(12) Li, X. L.; Wang, H. L.; Robinson, J. T.; Sanchez, H.; Diankov, G.; Dai, H. J. *J. Am. Chem. Soc.* **2009**, *131*, 15939–15944.
(13) Wei, D. C.; Liu, Y. Q.; Wang, Y.; Zhang, H. L.; Huang, L. P.; Yu, G. *Nano Lett.* **2009**, *9*, 1752–1758.
(14) Romero, H. E.; Shen, N.; Joshi, P.; Gutierrez, H. R.; Tadigadapa, S. A.; Sofo, J. O.; Eklund, P. C. *ACS Nano* **2008**, *2*, 2037–2044.
(15) Carvajal, J. J. *MRS Bull.* **2009**, *34*, 475–476.
(16) Xiao, K.; Liu, Y. Q.; Hu, P. A.; Yu, G.; Sun, Y. M.; Zhu, D. B. *J. Am. Chem. Soc.* **2005**, *127*, 8614–8617.
(17) Qu, L. T.; Liu, Y.; Baek, J. B.; Dai, L. M. *ACS Nano* **2010**, *4*, 1321–1326.
(18) Czerw, R.; Terrones, M.; Charlier, J. C.; Blase, X.; Foley, B.; Kamalakaran, R.; Grobert, N.; Terrones, H.; Tekleab, D.; Ajayan, P. M.; Blau, W.; Ruhle, M.; Carroll, D. L. *Nano Lett.* **2001**, *1*, 457–460.
(19) Yang, Q. H.; Xu, W. H.; Tomita, A.; Kyotani, T. *J. Am. Chem. Soc.* **2005**, *127*, 8956–8957.
(20) Sui, Y.; Appenzeller, J. *Nano Lett.* **2009**, *9*, 2973–2977.
(21) Long, D. H.; Li, W.; Ling, L. C.; Miyawaki, J.; Mochida, I.; Yoon, S. H. *Langmuir* **2010**, *26*, 16096–16102.
(22) Qian, W.; Hao, R.; Hou, Y. L.; Tian, Y.; Shen, C. M.; Gao, H. J.; Liang, X. L. *Nano Res.* **2009**, *2*, 706–712.
(23) Peng, Y. L.; Ma, C. Y. *Application Handbook of Supercritical Fluid Technology*; Chemical Industry Press: Beijing, China, 2005.
(24) Serhatkulu, G. K.; Dilek, C.; Gulari, E. *J. Supercrit. Fluids* **2006**, *39*, 264–270.
(25) Gulari, E.; Serhatkulu, G. U.S. patent 7 157 517, Jan 2, 2007.
(26) Ruthven, D. M. *Encyclopedia of Separation Technology*; John Wiley: New York, 1997.
(27) Kiran, E.; Peters, C.J.; Debenedetti, P. G. *Supercritical Fluids-Fundamentals for Applications*; Klüwer Academic Publishers: Dordrecht, The Netherlands, 1994.
(28) Pu, N. W.; Wang, C. A.; Sung, Y.; Liu, Y. M.; Ger, M. D. *Mater. Lett.* **2009**, *63*, 1987–1989.

(29) Bengelsdorf, I. S. *J. Am. Chem. Soc.* **1958**, *80*, 1442–1444.
(30) Bengelsdorf, I. S. *J. Org. Chem.* **1963**, *28*, 1369–1372.
(31) Forsberg, J. H.; Spaziano, V. T.; Balasubramanian, T. M.; Liu, G. K.; Kinsley, S. A.; Duckworth, C. A.; Poteruca, J. J.; Brown, P. S.; Miller, J. L. *J. Org. Chem.* **1987**, *52*, 1017–1021.
(32) Nevidomskyy, A. H.; Csanyi, G.; Payne, M. C. *Phys. Rev. Lett.* **2003**, *91*, 105502.
(33) Ronning, C.; Feldermann, H.; Merk, R.; Hofsass, H.; Reinke, P.; Thiele, J. U. *Phys. Rev. B* **1998**, *58*, 2207–2215.
(34) Yang, D.; Velamakanni, A.; Bozoklu, G.; Park, S.; Stoller, M.; Piner, R. D.; Stankovich, S.; Jung, I.; Field, D. A.; Ventrice, C. A.; Ruoff, R. S. *Carbon* **2009**, *47*, 145–152.
(35) Akhavan, O.; Ghaderi, E. *J. Phys. Chem. C* **2009**, *113*, 20214–20220.
(36) Gammon, W. J.; Kraft, O.; Reilly, A. C.; Holloway, B. C. *Carbon* **2003**, *41*, 1917–1923.
(37) Nakayama, Y.; Soeda, F.; Ishitani, A. *Carbon* **1990**, *28*, 21–26.
(38) Dresselhaus, M. S.; Eklund, P. C. *Adv. Phys.* **2000**, *49*, 705–814.
(39) Ferrari, A. C.; Meyer, J. C.; Scardaci, V.; Casiraghi, C.; Lazzeri, M.; Mauri, F.; Piscanec, S.; Jiang, D.; Novoselov, K. S.; Roth, S.; Geim, A. K. *Phys. Rev. Lett.* **2006**, *97*, 187401.
(40) Bai, J. W.; Zhong, X.; Jiang, S.; Huang, Y.; Duan, X. F. *Nat. Nanotechnol.* **2010**, *5*, 190–194.
(41) Akhavan, O. *Acs Nano* **2010**, *4*, 4174–4180.